Visualization Methods for Assisting Detection of Cardiovascular Neuropathy

David J. Cornforth[1], Mika P. Tarvainen[2], and Herbert F. Jelinek[3]

Abstract— **Visualization models can assist in understanding the complex pattern of disease, where the signs may be buried in complex data. In this work we propose a new method for visualization of data derived from Heart Rate Variability (HRV) analysis, to indicate whether a person has developed, or is developing, signs of definite Cardiac Autonomic Neuropathy (CAN). Here, the visualizations are compared with actual data recorded from people attending a diabetes clinic with and without definite CAN. Indications from the new visualization technique are compared to the results of established diagnostic measures using the Ewing battery of tests. We find the proposed method to offer useful insights into this disease, as rather than relying upon a binary yes/no decision, it offers a comprehensive picture of the complexity of this disease.**

I. Introduction

Visualization of multi-feature clinical data requires a comprehensive design process for the development of an integrated display, which is effective, informative and enhances clinical decision making [1]. Visualization is a function of available diagnostic trends and aesthetics, which requires transposition from one or many data sources, and combines disparate data into a workable presentation [2]. Multigraphs, sparklines or box plots are some approaches, which allow representation of co-varying features while showing normal ranges for test results [3]. In clinical practice, new results from many sources are generated systematically over time, depending on the patient and treatment protocol, and require correct interpretation and follow-up. Appropriate visualization of this complex data allows easy comparison between patient reviews over a period of time. Visualization of multi-domain clinical data can also be interactive and multi-dimensional, but for all types of visualization, the most important aspects are that they promote exploration of the data, promote easy monitoring, and lead to the discovery of insights of relevance for the patient as well as for the clinician [4].

Cardiac Autonomic Neuropathy (CAN) is a disease that involves nerve damage. This leads to abnormal control of the heart rate, and is therefore potentially detectable using Heart Rate Variability (HRV). CAN disrupts the normal rhythm modulation of the heart, and may manifest in arrhythmias and heart attack. Early detection of CAN has the potential to improve treatment outcomes. In previous work [5], [6] we have shown that advanced measures of HRV entropy can be useful in detecting CAN. Here we extend this work by providing a new visualization technique to assist clinicians in interpreting multi-feature HRV results.

HRV is well known as an indicator of the regulation of the heart [7]. A typical ECG signal is shown in Figure 1. The most reliable feature that can be obtained from such a signal is the interval between successive R peaks, known as the RR interval, or inverse of the heart rate. This is used to determine HRV.

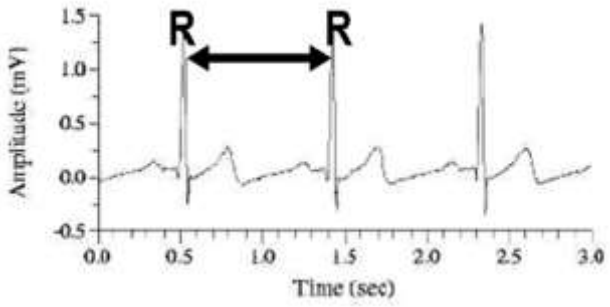

Figure 1. Normal ECG recording showing RR interval.

The natural rhythm of the human heart is subject to variation that is believed to indicate the health of the cardiovascular system, in that too much or too little variability between beats increases the risk of arrhythmia [8]. RR intervals are obtained from the recorded ECG and subjected to further analysis through a variety of algorithms in order to yield variables with good discriminant power [7].

A. Time domain measures

Time domain measures include the mean and standard deviation of the RR intervals (SDNN) recorded. The number of pairs of successive intervals that differ by more than 50ms, divided by the total number of intervals, yields a parasympathetic measure (pNN50%). The Root Mean Square of Successive Differences (RMSSD) and the triangular index (Triang. index) are also parasympathetic measures. The triangular interpolation of the interval histogram (TINN) is the estimated width of the density distribution. This is believed to be sensitive to physical and emotional load, or to the intensity of the sympathetic nervous system tone.

The Poincaré plot is a visual representation of the time series and is constructed by plotting each consecutive RR interval as a point where $y = RR(t)$ and $x = RR(t-1)$. From this plot a fitted ellipse leads to estimating SD1 (short term correlation) and SD2 (long term correlation) [10], [11]

[1]D Cornforth is with the Applied Informatics Research group, University of Newcastle, Australia, and the School of Engineering and Information Technology, University of New South Wales, Canberra, Australia, phone: +612 4985 4069, email: David.Cornforth@newcastle.edu.au

[2]M Tarvainen is with the Department of Applied Physics, University of Eastern Finland, Kuopio, Finland and Department of Clinical Physiology and Nuclear Medicine, Kuopio University Hospital, Kuopio, Finland.

[3]H Jelinek is with the Centre for Research in Complex Systems and School of Community Health, Charles Sturt University, Albury, Australia.

978-1-4244-7929-0/14/$26.00 ©2014 IEEE

(Figure 2). An extension is the Recurrence Plot, which represents a sequence of length n as a point in n-dimensional space, then represents similar pairs as points on a two-dimensional space. The Recurrence Rate (REC) is the density of these similar points, Determinism (DET) is the percentage of recurring points, identified by diagonal lines, and Lmean is the mean length of diagonal lines exceeding a threshold.

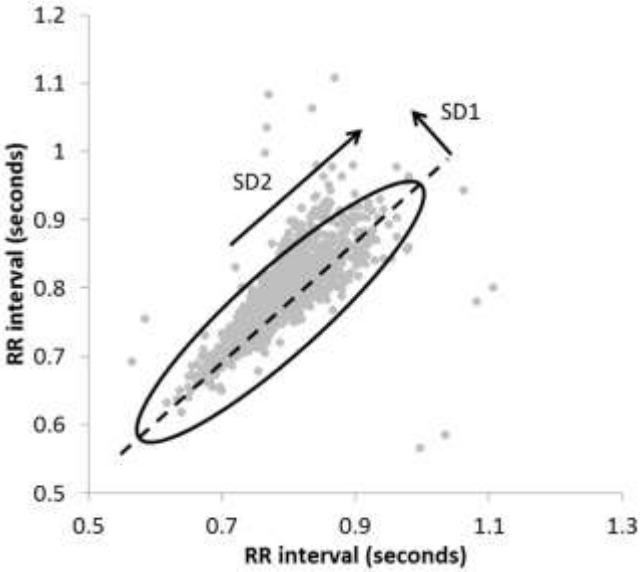

Figure 2. Poincaré plot for a sequence of RR intervals allows the estimation of SD1 and SD2.

B. *Frequency domain methods*

Frequency domain methods divide the spectral distribution into very low, low and high frequency regions (Figure 3). Low frequency power (LF) is believed to be indicative of both parasympathetic and sympathetic activity. High frequency (HF) is indicative of parasympathetic activity. Very Low Frequency (VLF) amplitude is closely connected with psycho-emotional state and functional condition of the brain [11]. Other work [12] has shown the important meaning of VLF - range analysis, and that the capacity of VLF fluctuations of HRV is a sensitive indicator of management of metabolic processes and reflects deficit energy states. The ratio of low to high frequency components, which is indicative of sympathovagal balance, may also be calculated as well as the total power [7]. A component may also be divided by the total power, to express it in normalized units (n.u.).

C. *Non-linear measures*

Non-linear measures include Detrended Fluctuation Analysis (DFA), fractal dimension, symbolic dynamics and entropy measures such as Sample Entropy and Renyi Entropy. DFA is an estimate of the fractal correlation of the RR interval series, and provides an exponent expressing short-term correlations (alpha1), and another expressing long-term correlations (alpha2). The correlation dimension (D2) of fractal analysis was also used. Renyi entropy H is a generalization of the Shannon entropy:

$$H_\alpha(X) = \frac{1}{1-\alpha} log_2 \left(\sum_{i=1}^{n} p_i^\alpha \right)$$

where p_i is the probability that $X = x$ and α is the order of the entropy measure. This is the parameter that is varied to produce the multiscale entropy.

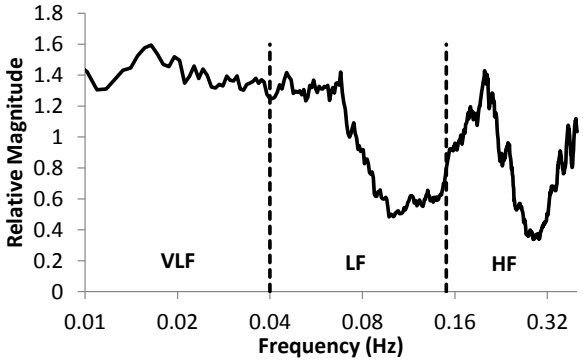

Figure 3. Power spectrum of RR intervals showing VLF, LF and HF regions.

HRV analysis associated with CAN has as yet not been investigated for multi-feature visualization, despite literature on HRV analysis covering some twenty or more features [13], [8]. The Poincare Map or the Power Spectrum distribution, as shown in Figure 2 and 3, are common visualizations of HRV, but are restricted to comparing two or three HRV measures.

II. METHODOLOGY

A. *Participants*

Participants were recruited from those attending the screening clinic as part of the Charles Sturt Diabetes Complications Screening Group (DiScRi), Australia [14]. All participants provided a 20-minute recording using lead II ECG, from which the RR intervals were extracted. The same physical conditions were used for each participant, and all subjects were comparable for age, gender, and heart rate. Participants were screened to exclude those with severe heart disease, presence of a pacemaker, kidney disease or polypharmacy, including multiple anti-arrhythmic medication. The study was approved by the Charles Sturt University Human Ethics Committee and written informed consent was obtained from all participants.

B. *CAN Classification*

The participants, 11 with definite CAN and 71 without CAN, were identified using the Ewing battery [15] of tests [16], [17]. From the 20-minute ECG recording, a 15-minute segment was taken from the middle to avoid start-up, ending and movement artefacts in the recording. Only the RR intervals were retained, and no other information from the ECG was utilized in this study. RR intervals were normalized by subtracting the mean value from the RR data. A variety of

measures, as discussed above, were extracted. The multiscale Renyi entropy was calculated using $-5 < \alpha < +5$, where $\alpha = 1$ is the Shannon entropy and $\alpha = 2$ is the squared entropy. Sample Entropy was also calculated in order to provide a comparison.

C. HRV Feature Visualization

All features calculated from HRV were visualized using a Spider diagram. Preparation of such a diagram requires some care. The various measures must be normalized to allow all of them to fit into a comparable range. Deviation from the mean is not suitable, as it cannot be assumed that the distributions of these variables are Gaussian. Alternatively each measure may be related to the percentiles of its distribution. Some variables will extend beyond the normal range in a positive direction, while others will extend in a negative direction, so the scale must be adjusted to allow this to be visible.

The measure chosen is the rank of the variable. For values falling above or below the range of the Normal group, the rank was allocated the value of 1.1 or -0.1 respectively. For example, patient *i* has a value of 6.6 for RMSSD. As the normal range is from 8.3 to 173, this patient has an RMSSD that is completely outside the normal range, and is given a score of -0.1. These ranks are plotted in the spider diagrams used here.

III. RESULTS

Spider diagrams were produced for the 11 patients diagnosed with Definite CAN. Examples are provided to illustrate the possible presentations of definite CAN, using this multi-feature HRV visualization. Figure 4 shows one of the subjects from the Definite group that appears to diverge the least from the Normal group. The thick black lines provide the 25th and 75th percentile for the Normal group. The subject with definite CAN is shown using the dotted line.

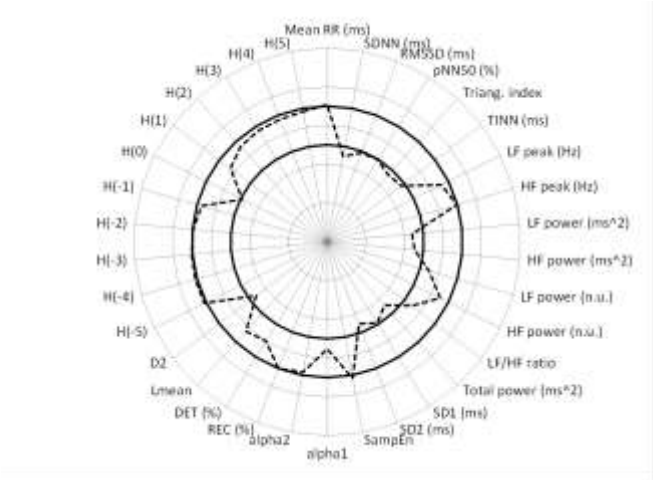

Figure 4. Spider diagram from a person with Definite CAN, showing a low relative deviation from the Normal group.

Notice that for nearly every measure used, this person received a score that placed them near the 25th or the 75th percentile. The spider diagram includes results of steady-state measures such as SDNN and total power, as well as the composition of HRV rhythms reflecting different regulatory mechanisms (high and low frequency power). The same diagram allows comparison with nonlinear methods that measure the extent to which interbeat intervals are correlated (correlation dimension D2), and Detrended Fluctuation Analysis (DFA). The latter indicates the internal short-term and long-term correlation within the signal. Also included are entropy measures, which are indicators of the regularity or complexity of the signal. In Figure 4, the total variance of the signal, as measured by SDNN or total power (TP), is low. LF and HF power are also low. D2 indicates that RR intervals are not highly correlated and this may be the reason that entropy measures such as SampEn and the Renyi entropies are near the upper limit of normal. For definite CAN, one would expect low HF, as CAN results in reduced parasympathetic contribution. This observation applies to other features as well, such as alpha1 (a DFA measure) and SD1 (Poincaré mapping), which indicate low short-term correlation and are associated with the parasympathetic component of the ANS. This type of presentation is often seen in post myocardial infarct patients and indicates in this case extensive loss of normal autonomic nervous system modulation.

Another subject with Definite CAN is shown in Figure 5. All HRV features show a higher deviation from the Normal group than the previous example.

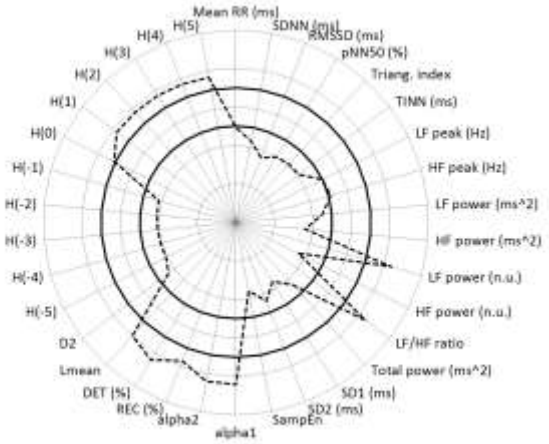

Figure 5. Spider diagram from a person with Definite CAN, showing a high relative deviation from the Normal group.

The time and frequency domain results seem to trend similarly to figure 4, indicating parasympathetic withdrawal. The interesting aspect of Figure 5 is that the negative Renyi features are outside the normal range but in the opposite direction to the positive values. Renyi entropies show continuity properties with respect to their scaling exponent α and thus in the case of Figure 5, the complexity content with respect to the Renyi scaling exponents differ dramatically compared to the patient shown in Figure 4. This may be a reflection of the high DFA alpha1 and alpha2 values, which indicates that the internal correlations of the signal are moving towards a Brownian noise type of pattern and therefore abnormal.

These results should be viewed in the context of current accepted methods for detection of CAN – in this case the gold standard is the Ewing battery. According to that test, definite CAN is indicated by any two of three heart rate parameters being abnormal (Valsalva, deep breathing or lying to standing) plus one of the two BP measures (handgrip or lying to standing). This leads to two important points.

First, each of the Ewing measures has a different weighting in terms of its association with CAN. Second, Ewing tests are influenced by patient compliance. Thus a frail elderly person or someone with arthritis is more likely to have an abnormal handgrip result. It is customary to omit a Valsalva test if there is known respiratory or cardiac disease, but asymptomatic respiratory disease or seasonal asthma may also affect deep breathing and Valsalva results. Therefore the current spider diagram visualization obtained from patients in a passive supine position may be a more robust way of determining CAN than the Ewing battery. In addition this multi-feature representation provides a good overview of the different HRV features, which have different properties and thus can be interpreted as a combined feature set.

IV. Conclusion

In this paper we have presented a new visualization technique for the results of HRV. One advantage of this type of representation is that it alerts to the fact that it is not only when certain HRV features are lower than normal but also when they are higher than normal that pathophysiology is expected. The Spider diagrams indicate that there is no simple representation of definite CAN pathology but that there is a complex relationship between global steady-state characteristics, frequency specific rhythms of the biosignal, internal short and long-term correlations between RR intervals and the complexity of the system.

In future work we may be able to improve the definition of the Normal group by considering age and identifying the strongest HRV features for classification. In this work we have shown the utility of visualizing HRV features with a spider diagram in clinical practice, where it is important to be able to make a decision based on multi-feature input in a timely and optimal manner.

References

[1] Erbacher, R. F. (2007). Exemplifying the Inter-Disciplinary Nature of Visualization Research, Proceedings of IV07: 11th International Conference Information Visualisation (pp. 623-630). Zurich, Switzerland

[2] Jelinek, H. F., Cornforth, D. J. & Blackmore, K. (2011) Visualisation in biomedicine as a means of data evaluation. Journal of Visualization 14(4): 353-359

[3] T. Torsvik, B. Lillebo, and G. Mikkelsen, "Presentation of clinical laboratory results: an experimental comparison of four visualization techniques," Journal of the American Medical Informatics Association, October 6, 2012

[4] B. Schneiderman, C. Plaisant, and B. W. Hesse, "Improving health and healthcare with interactive visualization methods," HCIL Technical Report, vol. 1, pp. 1-13, 2013

[5] David J Cornforth, Mika P Tarvainen and Herbert F Jelinek (2013) Using Renyi Entropy to Detect Early Cardiac Autonomic Neuropathy, Proceedings of the 35th Annual International Conference of the IEEE Engineering in Medicine and Biology Society, July 3 - July 7, 2013 (EMBC'13), Osaka Convention Center, Osaka, Japan.

[6] Jelinek, H.F., Tarvainen, M.P. and Cornforth, D.J. (2012) Renyi entropy in identification of cardiac autonomic neuropathy in diabetes, Proceedings of the Conference on Computing in Cardiology (CinC), Krakow, pp. 909 - 912, ISBN 978-1-4673-2076-4.

[7] Task Force of the European Society of Cardiology (TFESC), North American Society of Pacing Electrophysiology, Heart Rate Variability: Standards of Measurement, Physiological Interpretation, and Clinical Use, Circulation 93 (1996) 1043-1065.

[8] A. Voss, S. Schulz, R. Schroeder, M. Baumert, and P. Caminal, "Methods derived from nonlinear dynamics for analysing heart rate variability," Philosophical Transactions of the Royal Society A: Mathematical, Physical and Engineering Sciences, vol. 367, pp. 277-296, January 28, 2009 2009

[9] M.P. Tulppo, T H. Makikallio, T E. Takala, T. Seppanen, H.V. Huikuri, Quantitative beat-to-beat analysis of heart rate dynamics during exercise, American journal of Physiology - Heart 271(1) (1996) H244-H252.

[10] C.K. Karmakar, A.H. Khandoker, A. Voss, M. Palaniswami, Sensitivity of temporal heart rate variability in Poincaré plot to changes in parasympathetic nervous system activity, BioMedical Engineering OnLine 10(17) (2011) Available at http://www.biomedical-engineering-online.com/content/10/1/17, accessed Dec 2012.

[11] R.M. Baevsky, A.P. Berseneva, Use of Kardivar System for Determination of the Stress Level and Estimation of the Body Adaptability, (2008) available at www.ehrlich.tv/Kardivar_Methodical_Eng.pdf, accessed Dec 2012.

[12] A.N. Fleishman, Slow hemodynamic oscillations. The theory, practical application in clinical medicine and prevention. Novosibirsk: Nauka, 1999.

[13] M. Risk, V. Bril, C. Broadbridge, and A. Cohen, "Heart rate variability measurement in diabetic neuropathy: review of methods," Diabetes Technology and Therapeutics, vol. 3, pp. 63-76, 2001;

[14] H.F. Jelinek, C.Wilding and P. Tinley. An innovative multi-disciplinary diabetes complications screening programme in a rural community: A description and preliminary results of the screening. Australian Journal of Primary Health Vol. 12, 2006, pp. 14-20.

[15] Ewing DJ, Clarke BF. Diabetic autonomic neuropathy: present insights and future prospects. Diabetes Care. 1986; 9: 648–665.

[16] M. Javorka, Z. Trunkvalterova, I. Tonhajzerova, J. Javorkova, K. Javorka and M. Baumert. Short-term heart rate complexity is reduced in patients with type 1 diabetes mellitus. Clin Neurophysiol Vol. 119, 2008, pp. 1071-81.

[17] A.H. Khandoker, H.F. Jelinek and M. Palaniswami. Identifying diabetic patients with cardiac autonomic neuropathy by heart rate complexity analysis. Biomed Eng Online. Vol. 8, 2009.